GSA Data Repository 2019145

Accommodation- vs. supply-dominated systems for sediment partitioning to deep water

Supplementary documents

Jinyu Zhang[1], Wonsuck Kim[1], Cornel Olariu[1,2], Ronald Steel[1,3]

1. Jackson School of Geosciences, University of Texas at Austin, Texas, USA

2. National Institute for Marine Geology and Geoecology, Bucharest, Romania

3. Heriot-Watt University, Edinburgh, UK

1. Modeling shoreline migration over shelf-margin clinoform
2. Animations showing shoreline migration in Figs. 1C and 1D
   (Also see attached AVI file: 2019145_Animation DR1.avi)
3. Modeled results of Fig. 2
4. Inputs of three ancient systems in Fig. 3B
5. References

1. Modeling shoreline migration over shelf-margin clinoform

We modified the geometric model in Kim et al. (2009) to model shoreline position along a dip-oriented cross section. The model assumes a deltaic clinoform prograding over basement. The deltaic clinoform has a fixed topset gradient (S_t), 0.01° and foreset gradient (S_f), 3°. Its topography, η, can be described as

$$\eta = \eta_s + (s - x)\tan(S_t) \text{ if } x<s \text{ [S1a]}$$

$$\eta = \eta_s - (x - s)\tan(S_f) \text{ if } x>s \text{ [S1b]}$$

Where η_s is the elevation at shoreline, *s* is the shoreline location. A preexisting shelf-margin clinoform is now used as initial basement (Fig. 1). The elevation at shoreline, η_s, equals to the sea level (*z*). The sea level varied through simulated model time (t in My) (Equation S2).

$$z = A\sin(2\pi\left(\frac{t}{T}\right)) \text{ [S2]}$$

Where A is the amplitude of sea-level change and T is the frequency of sea-level change. 5% of the deposits in each eustatic cycle are eroded during sea-level fall, and this contributes to the increasing sediment supply at the lowest sea-level point. The amount of eroded deposits (i.e., 5%) is chosen based on the examples in both Holocene and experimental studies (Blum and Tornqvist, 2000; Martin et al., 2011). The shelf gradient (*a in °*) is estimated by shelf width (*W in km*) based on the empirical relationship (Equation S3) obtained from 32 modern shelves (Zhang et al., 2017). The height of the shelf-margin clinoform is assumed to be 0.5 km. The slope gradient is fixed as 3° and the basin floor is assumed to be flat. Therefore the topography of basement, *b*, is as Equation S4.

$$\alpha = 3.2561W^{-0.851} \text{ [S3]}$$

$$b = -x\tan(\alpha)\ if\ x \le W \text{ [S4a]}$$

$$b = -W tan(\alpha) - (x - W)\tan(3°)\ if\ x > W \text{ [S4b]}$$

$$b = -0.5 - W tan(\alpha)\ if\ b < -0.5 - W tan(\alpha)\ [S4c]$$

The mass balance along a sedimentary basin from x=0 to x=L is expressed as

$$q_s t = \int_0^L (\eta - b) dx\ [S5]$$

Where q_s is the sediment supply (km^2/My), and L denotes total length of the basin. The shoreline position (s, z) can be solved numerically for each time step (i.e., 0.005 My) integrating Equation S1-5.

We estimate the deep-water proportion of total sediment supply in order to compare the efficiency of different sediment dispersal systems. The deepwater sediment proportion is calculated in the final stratigraphy of modeled results by Equation S6.

$$P_{dw} = \frac{V_{dw}}{q_s t}\ [S6]$$

Where P_{dw} is the deep-water sediment proportion; V_{dw} is the deep-water volume partitioning into the deep water (i.e., sediments basinward from the shelf edge).

Natural systems are more complicated than the simplified model used here. We list a few limitations of the employed model below, possibly providing future research opportunities for source-to-sink studies. Firstly, expanding the present 2D model to a full 3D model is desirable, but would need a better understanding on the amount of sediment brought by longshore drift in and out of the system (see also Liu et al., 2017) and also the sediment routing as deltas prograde towards the shelf edge or canyon head. For example, an upstream avulsion could divert a river far from the pre-existing canyon head, which diminishes more effective sediment delivery to deep water. Secondly, the gradients of shelf and delta topset are fixed in the model. In nature, these gradients are controlled by the upstream factors (Whipple et al. 1998) and downstream conditions (Carlson et al. 2018). Variation of the gradients caused by the upstream boundary conditions can generate topset erosion and/or deposition even without sea-level change, thus modifying the sediment profile. Thirdly, even though the sediment supply is assumed to be constant here, climate-induced sediment supply cycles (<1 My) may be in phase or out of phase with sea-level change (van den Berg van Saparoea and Postma, 2008; Zhang et al., 2016). The influence of cyclic sediment supply on sediment dispersal to deep water is a good future research topic.

2. Animations showing shoreline migration in Figs. 1C and 1D

See attached AVI file 'Shoreline migration' for an animation showing the shoreline migration for one accommodation-dominated system (Fig. 1C) and one supply-dominated system (Fig. 1D). The red points indicate the shoreline positions landward from the shelf edge whereas the green points indicate the shoreline positions basinward from shelf edge.

3. Modeled results of Fig. 2

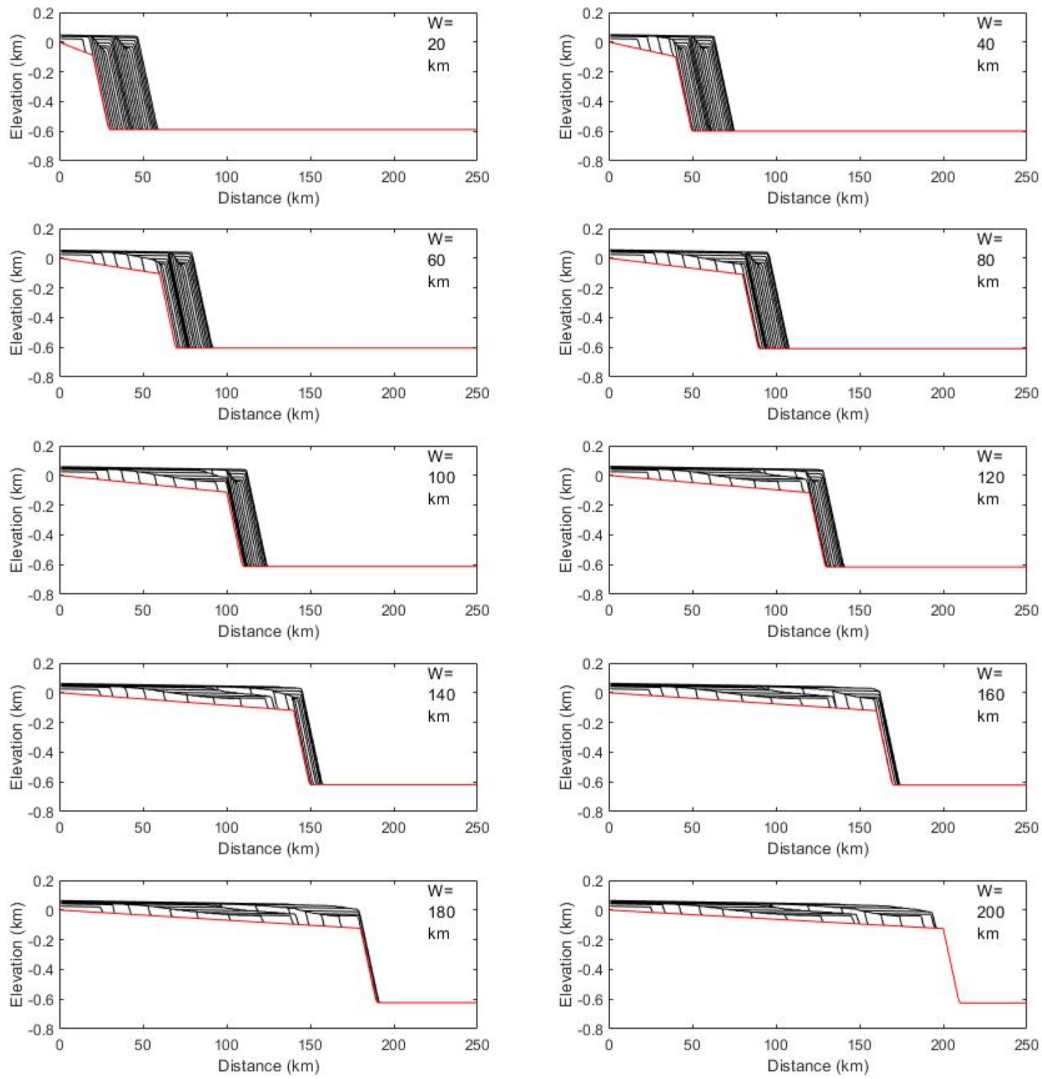

Figure S1. Black examples in Fig. 2B (A=40 m; T=0.45 My; W varied from 20-200 km). A/T: amplitude and frequency of sea-level change; W: shelf width

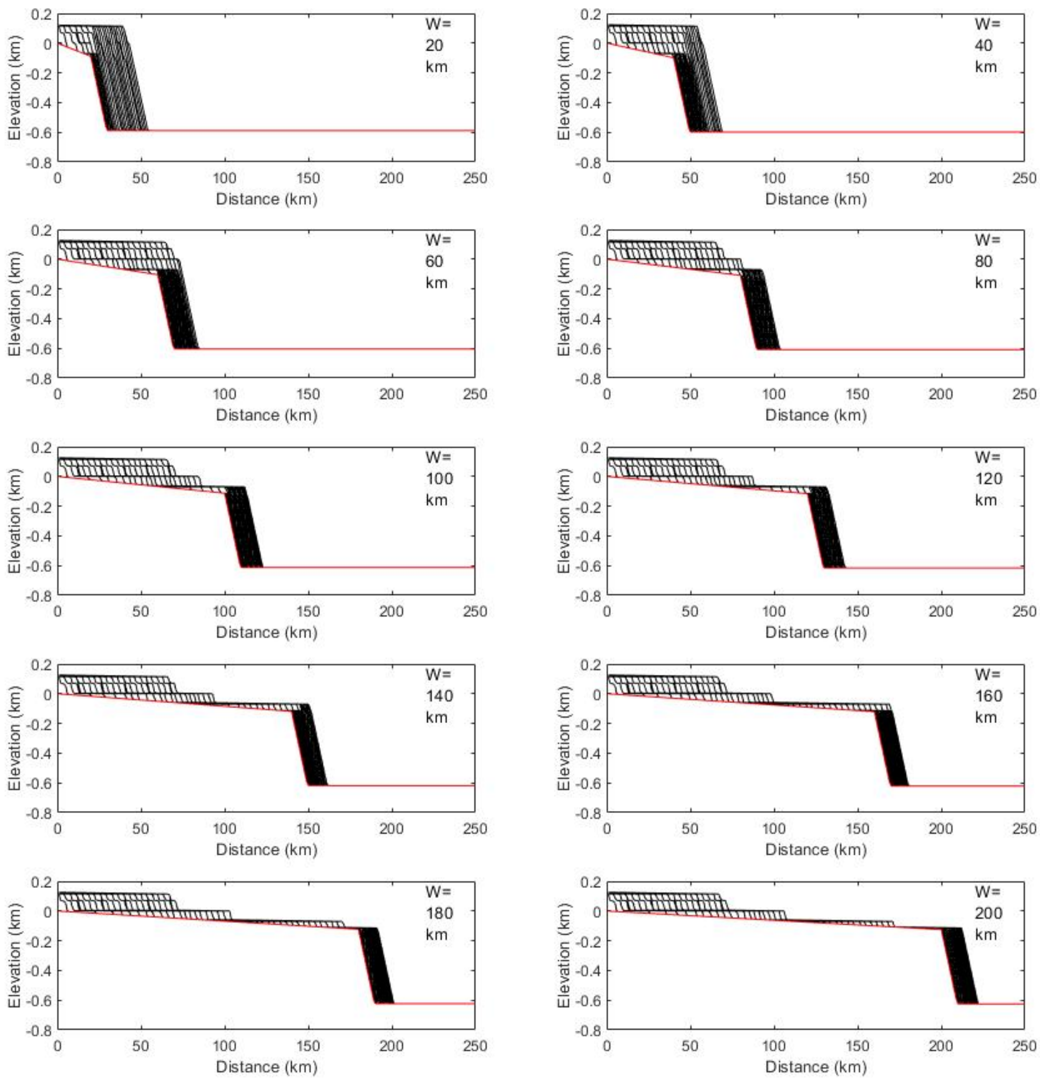

Figure S2. Red examples in Fig. 2B (A=120 m; T=0.05 My; W varied from 20-200 km). A/T: amplitude and frequency of sea-level change; W: shelf width.

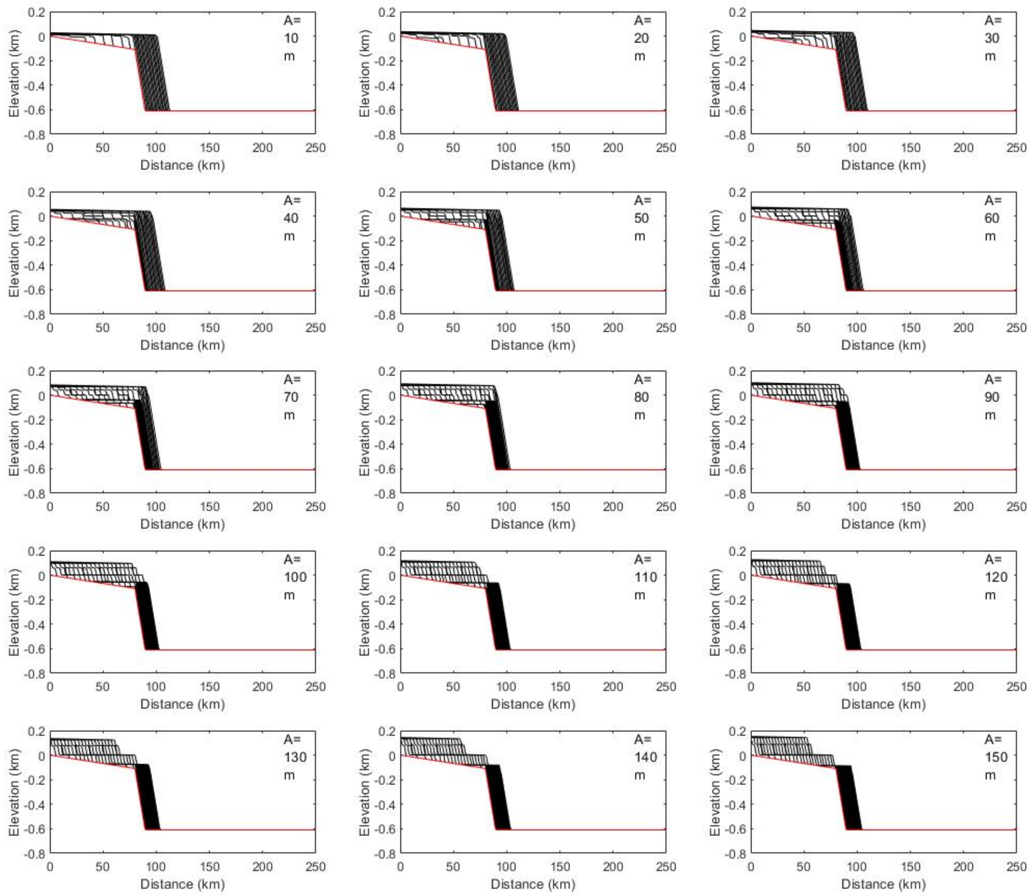

Figure S3. Black examples in Fig. 2C (W=80 Km; T=0.05 My; A varied from 0-150 m). A/T: amplitude and frequency of sea-level change; W: shelf width.

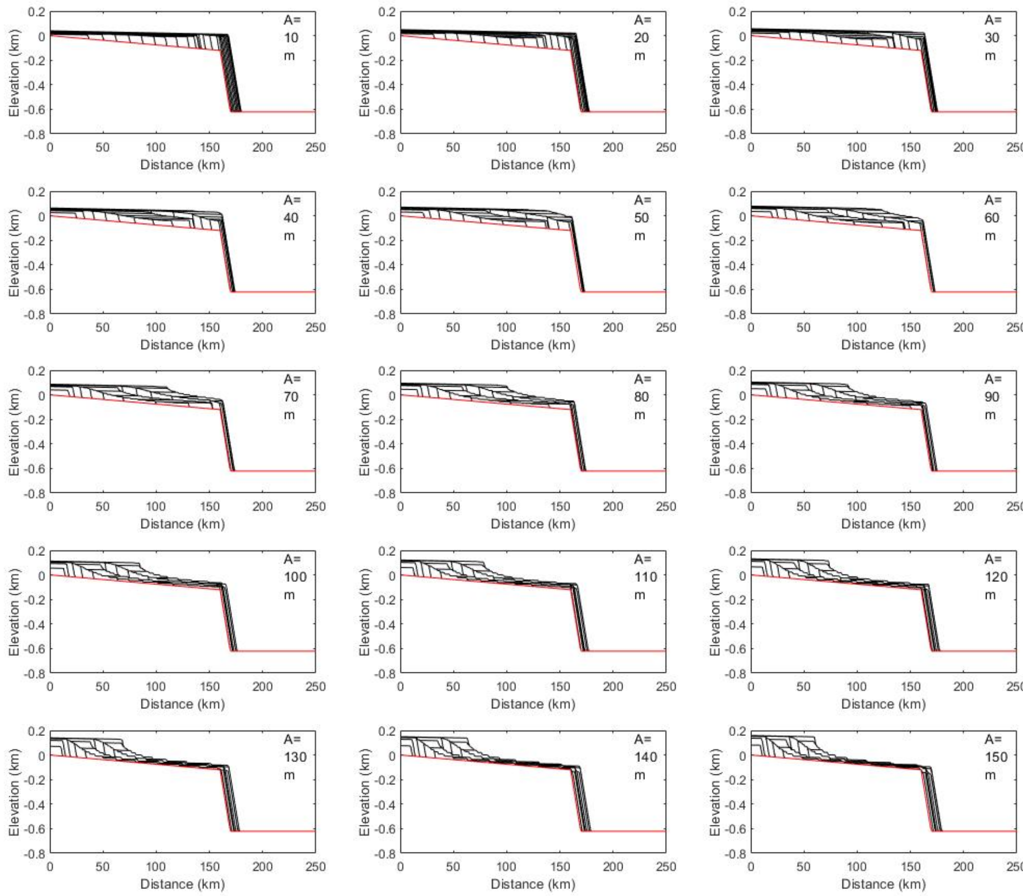

Figure S4. Red examples in Fig. 2C (W=160 Km; T=0.45 My; A varied from 0-150 m). A/T: amplitude and frequency of sea-level change; W: shelf width.

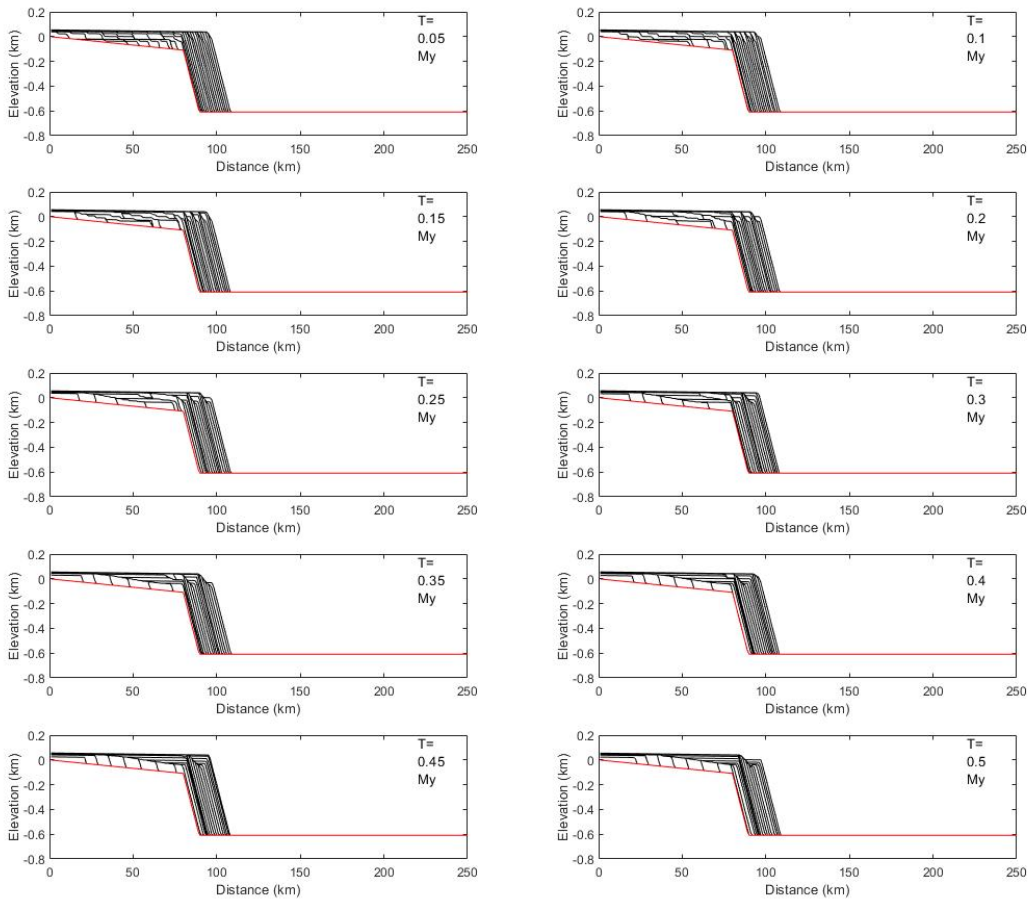

Figure S5. Black examples in Fig. 2D (W=80 Km; A=40 m; T varied from 0.05-0.5 My). A/T: amplitude and frequency of sea-level change; W: shelf width.

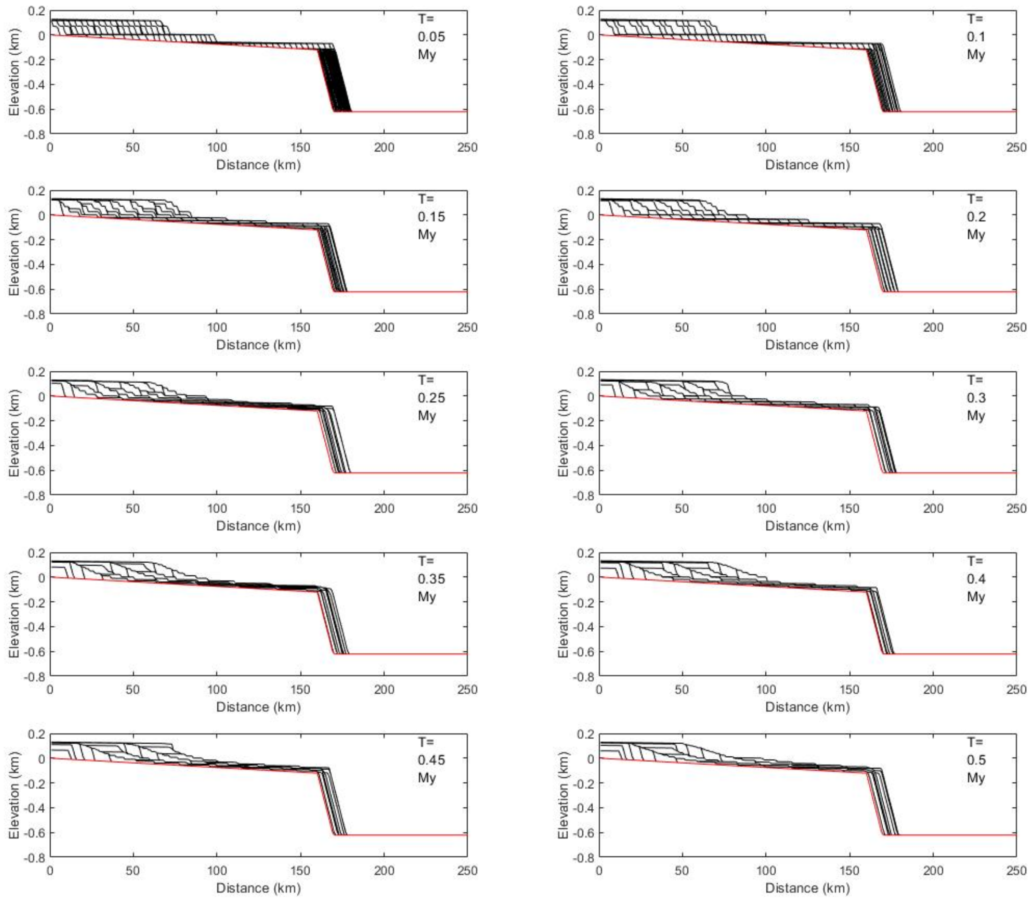

Figure S6. Red examples in Fig. 2D (W=160 Km; A=120 m; T varied from 0.05-0.5 My). A/T: amplitude and frequency of sea-level change; W: shelf width.

4. Inputs for three ancient systems in Fig. 3B

System	Clinoform Number	Shelf width (km)	Amplitude of sea-level change (m)*	Simplified shelf accommodation (km^2)	Total sediment supply (km^2)	SASR	References
Maastrichtian Washakie**	12	14	40	0.84	5.59	0.114	Carvajal and Steel, 2012
	11	38	40	1.16	5.49	0.348	
	10	38	40	1.95	7.93	0.262	
	9	45	40	2.21	4.31	0.230	
	8	61	40	2.43	7.88	0.308	
	7	55	40	1.81	7.90	0.513	
	6	49	40	1.51	5.75	0.246	
	5	29	40	1.51	4.33	0.212	
	4	21	40	0.56	4.89	0.150	
Pliocene Orinoco	13	42	120	5.04	19.99	0.252	Chen et al., 2018a, 2018b
	12	41	120	4.92	7.79	0.632	
	11	39	120	4.68	8.00	0.585	
	10	37	120	4.44	6.22	0.713	
	9	31	120	3.72	9.04	0.411	
	8	29	120	3.48	3.70	0.942	
	7	28	120	3.36	10.46	0.321	
	6	18	120	2.16	7.69	0.281	
	5	14	120	1.68	8.54	0.197	

	4	13	120	1.56	3.81	0.409	
Miocene	m3-2.2	160	120	19.20	16.00	1.200	Steckler et al., 1999;
New Jersey	m4-3	160	120	19.20	14.40	1.333	Hodgson et al., 2018
	m5-4	150	120	18.00	14.40	1.250	
	m5.2-5	150	120	18.00	5.95	3.025	
	m5.4-5.2	150	120	18.00	7.44	2.419	
	m5.6-5.4	150	120	18.00	11.25	1.600	
	m6-5.6	140	120	16.80	10.00	1.680	

* The amplitude of sea-level change in greenhouse and icehouse is assumed to be 40 m and 120 m respectively.

** The deltaic system width is measured as 80 km from Fig. 7.1 in Carvajal and Steel (2012).

Abbreviation: *SARS* = Shelf-accommodation/supply ratio

REFERENCES

Carlson, B., Piliouras, A., Muto, T. and Kim, W., 2018. Control of Basin Water Depth On Channel Morphology and Autogenic Timescales in Deltaic Systems. *Journal of Sedimentary Research*, *88*(9), pp.1026-1039.

Carvajal, C. and Steel, R., 2012. Source-to-Sink Sediment Volumes within a Tectono-Stratigraphic Model for a Laramide Shelf-to-Deep-Water Basin: Methods and Results. *Tectonics of Sedimentary Basins: Recent Advances*, pp.131-151.

Chen, S., Steel, R., Olariu, C. and Li, S., 2018a, Growth of the paleo-Orinoco shelf-margin prism: Process regimes, delta evolution, and sediment budget beyond the shelf edge. *GSA Bulletin*, *130*(1-2), pp.35-63.

Chen, S., Steel, R., Olariu, C. and Zhang, J., 2018b, Clinoform drivers of the Late Miocene to Pliocene paleo-Orinoco Delta. In EGU General Assembly Conference Abstracts, Vol. 20, p. 7910.

Hodgson, D.M., Browning, J.V., Miller, K.G., Hesselbo, S.P., Poyatos-Moré, M., Mountain, G.S. and Proust, J.N., 2018, Sedimentology, stratigraphic context, and implications of Miocene intrashelf bottomset deposits, offshore New Jersey. *Geosphere*, *14*(1), pp.95-114.

Liu, J.P., DeMaster, D.J., Nittrouer, C.A., Eidam, E.F. and Nguyen, T.T., 2017. A seismic study of the Mekong subaqueous delta: Proximal versus distal sediment accumulation. *Continental Shelf Research*, *147*, pp.197-212.

Kim, W., and 6 others, 2009, Net pumping of sediment into deep water due to base-level cycling: experimental and theoretical results. *External Controls on Deepwater Depositional Systems: SEPM, Special Publication*, *92*, pp.41-56.

Steckler, M.S., Mountain, G.S., Miller, K.G. and Christie-Blick, N., 1999, Reconstruction of Tertiary progradation and clinoform development on the New Jersey passive margin by 2-D backstripping. *Marine Geology*, *154*(1-4), pp.399-420.

van den Berg van Saparoea, A. P., and Postma, G., 2008, Control of climate change on the yield of river systems, in Hampson, G.J., et al., eds., Recent advances in models of siliciclastic shallow-marine stratigraphy: SEPM (Society for Sedimentary Geology) Special Publication 90, p. 15–33.

Whipple, K.X., Parker, G., Paola, C. and Mohrig, D., 1998, Channel dynamics, sediment transport, and the slope of alluvial fans: experimental study. *The Journal of Geology*, *106*(6), pp.677-694.

Zhang, J., Steel, R. and Ambrose, W., 2016, Greenhouse shoreline migration: Wilcox deltas. AAPG Bulletin, 100(12), pp.1803-1831.

Zhang, J., Steel, R. and Olariu, C., 2017, What conditions are required for deltas to reach the shelf edge during rising sea level?. *Geology*, *45*(12), pp.1107-1110.